Surface resonances on Ta(001)

Xiaohe Pan* and E. W. Plummer
Department of Physics, University of Pennsylvania, Philadelphia, Pennsylvania 19104-6396 and Laboratory for Research on the Structure of Matter, University of Pennsylvania, Philadelphia, Pennsylvania 19104-3859

M. Weinert
Department of Physics, Brookhaven National Laboratory, Upton, New York 11973-5000
(Received 21 May 1990)

We present a joint experimental and theoretical study of the electronic structure and surface resonances of the Ta(001) surface. Angle-resolved photoemission experiments were performed with use of synchrotron radiation in the photon-energy range 10 to 100 eV. Three surface resonances have been identified in the angle-resolved photoemission spectra. Their symmetry, dispersion, and orbital character are determined. The experimental data are compared to self-consistent local-density-functional calculations for 9- and 21-layer Ta(001) slabs that are either bulk terminated or have a 14% contraction of the surface interlayer spacing. Since the degenerate d states of bulk Ta (e.g., the $\Gamma_{25'}$ and Γ_{12} irreducible representations) are above the Fermi level, the spin-orbit interaction—which can lift orbital degeneracies—has little effect on the occupied bands and is not required in order to explain the behavior of the resonances. The calculations for the 14% contracted surface interlayer separation is in better agreement with the experimental result than are the bulk-terminated bands. The role of these surface resonances on the stability of the (001) face of Ta will be discussed.

I. INTRODUCTION

The (001) surfaces of bcc transition metals have a rich collection of surface electronic states. Previous studies of the (001) surfaces of transition metals have shown that the clean W(001) and Mo(001) surfaces go through a reversible phase transition from a (1×1) structure around room temperature to a $c(2\times2)$ structure at low temperature. While Ta(001) has the same crystal structure as W(001) and is a neighbor of W to the left in the Periodic Table, it does not reconstruct in a temperature range of 650–15 K.[1,2] The instability of the W(001) surface has been attributed to both surface-state nesting on the Fermi surface[3–5] and to a local rebonding of surface states.[6] For W(001) and Mo(001), three bands of occupied surface resonances have been observed. At the center of the Brillouin zone (BZ), two of the surface resonances are close to the Fermi level [0.2, 0.6 eV for W(001), and 0.2 and 0.8 eV for Mo(001)] and one low-lying surface resonance appears[7] at relatively higher binding energy (3.3 eV for W and 4.2 eV for Mo). The W(001) surface state at 0.6 eV binding energy at $\bar{\Gamma}$ crosses the Fermi level approximately[8] halfway along $\bar{\Gamma}\rightarrow\bar{M}$. This state has been suggested as the driving mechanism of the surface reconstruction.[3–6]

Few experimental studies of the Ta(001) surface have been reported. Bartynski and Gustafsson[9] have performed an inverse-photoemission (IPE) study of the unoccupied surface states on the Ta(001) surface. Two d-like surface states were observed above the Fermi level. Their energies and dispersions along $k_{\parallel}$ are in semiquantitative agreement with local-density calculations for a five-layer Ta(001) film.[10] Along $\bar{\Gamma}\rightarrow\bar{X}$ one of the surface resonances appears[9] to disperse below the Fermi level and should be visible near the $\bar{\Gamma}$ point in photoemission experiments.

From a study of the surface states of Ta(001) below the Fermi level, a more complete picture of Ta(001) can be obtained. To this end, an angle-resolved photoemission study of Ta(001) has been carried out using the polarized light from a synchrotron. We have carefully examined the electronic structure of the valence levels and the $4f$ core levels as a function of incident-photon energies, emission angles, and photon polarizations. Three surface resonances have been identified at the $\bar{\Gamma}$ point. (We will use the generic term "surface resonances" for surface-localized electron states in the bulk-projected gaps, as well as for those that overlap the bulk continuum.) They are located at about 0.0, 2.7, and 3.4 eV below the Fermi level. The dispersion of these surface resonances has been measured along both the $\bar{\Gamma}\rightarrow\bar{M}$ and $\bar{\Gamma}\rightarrow\bar{X}$ directions in the surface Brillouin zone (BZ). The resonances located at 0.0 and 2.7 eV binding energy are identified as mainly d_{z^2} in orbital character, and the one at 3.4 eV is composed of both d_{z^2} and $d_{x^2-y^2}$ orbitals. Polarization measurements have been used to verify the symmetry of the surface resonances, and photon-energy sweeps allow the identification of final states that couple the photon field to the surface resonances.

Relativistic local-density-functional (LDA) calculations of the valence bands of bulk Ta reveal that, *unlike W and Mo, inclusion of spin-orbit interaction causes only a small perturbation on the valence bands of Ta(001).* This can be attributed to the fact that the bands that are strongly

modified by the inclusion of spin orbit in W and Mo are now unoccupied for Ta(001). Thus spin-orbit interaction is not required to explain the behavior of these valence electronic states.

Total-energy calculations[11] for various surface-layer relaxations predict a contraction of the surface-interlayer separation of $\sim 13.2\%$ with respect to the lattice spacing of bulk Ta. This result is consistent with values determined from both low-energy electron diffraction[1] (LEED) and photoelectron-diffraction (PD) experiments.[12] We show the bands for both 0% (bulk termination) and 14% contractions of the first interlayer distance and *find that the surface electronic structure of Ta(001) is altered significantly by the surface relaxation.* Comparing to the results of our angle-resolved photoemission data for the number, position, dispersion, and symmetry of the surface resonances, good agreement is achieved for calculations with a 14% contraction.

II. EXPERIMENTAL DETAILS

A. Sample preparation

A mechanically polished and chemically cleaned single-crystal Ta(001) disk of 99.999% purity and approximately 6 mm in diameter is used as the sample for this angle-resolved photoemission study. Sharp x-ray diffraction patterns confirmed the ordered bulk structure of the Ta sample. The Ta(001) crystal is spot welded onto a tungsten wire and then mounted on an x-y-z linear and two-rotational manipulator. To clean the Ta(001) in the UHV chamber, repeated Ar-ion sputtering and high-temperature annealing techniques are employed. First, the sample is sputtered with 1-keV Ar ions for about 30 min to remove the contamination. Then the sample is electron bombarded from an adjacent hot filament, raising the temperature to about 2500 °C for 30 s. After several tens of cycles, a clean surface of Ta(001) is indicated by the ratio of the surface to bulk intensity, and the line shapes of the $4f$ core level, and sharp LEED patterns. For surface-sensitive work on reactive samples such as Ta(001), it is found that the ratio and line shapes of the $4f$ surface and bulk core levels are more sensitive to contamination and smoothness of the surface than other techniques such as Auger-electron spectroscopy and valence-band photoelectron spectroscopy. The large $4f$ surface core-level shift of 0.75 eV makes it easy to monitor the surface condition during the experiments.

B. Angle-resolved photoemission

The experiment was carried out at the National Synchrotron Light Source, beam line U12, at Brookhaven National Laboratory (Upton, NY). The photons from the uv storage ring are dispersed with a 15°-incidence toroidal grating monochromator. Photons in the energy range 10–100 eV are used to excite the photoelectrons from the Ta(001) surface. The spectra were taken with a 180° and 25-mm spherical energy analyzer with an acceptance of ±2.0°. The total-energy resolution in our investigation range varies from 0.1 to 0.5 eV. The experimental setup is arranged to allow the independent control of incidence and emission angles, so that one can either fix the photon-polarization vector and sweep $\mathbf{k}_{\parallel}$ or fix $\mathbf{k}$ and vary the polarization of $\mathbf{A}$. This setup allow us to map out the surface-state dispersion of Ta(001) along the $\bar{\Gamma}\rightarrow\bar{X}\rightarrow\bar{\Gamma}$ and $\bar{\Gamma}\rightarrow\bar{M}\rightarrow\bar{\Gamma}$ directions, with either s- or p-polarized incident photons. In order to compare the spectra taken at different photon energies and different times, the intensity of each energy-distribution curve taken by the spherical energy analyzer is normalized by the current from a reference W mesh.

The angle-resolved photoemission is performed in an UHV system with an operating pressure of 6×10^{-11} Torr. The exposure of the sample, mostly to hydrogen, was less than 0.1 L in 30 min [1 langmuir (L)$\equiv10^{-6}$ Torr sec]. Both valence and $4f$ core levels showed no contamination in that time. As a precaution, the sample was flashed cleaned every 20 min.

III. THEORETICAL DETAILS AND DISCUSSION

A. Relativistic effects on bulk Ta bands

Relativistic effects which modify the bands of heavy materials can be divided into two types: (1) those such as the mass-velocity and Darwin terms that shift bands, but do not cause any additional symmetry breaking, and (2) the spin-orbit interaction which changes the symmetry of the system and thus can introduce additional splitting and avoided crossings of levels. The symmetry-conserving relativistic terms are well described by the scalar relativistic approximation[13] (SRA) commonly used in electronic-structure calculations. In what follows, the term spin orbit will be reserved for the symmetry-breaking interactions alone; all other relativistic changes of the bands are already included via the SRA. (The differences between the SRA and nonrelativistic bands can be on the order of an eV, especially for s-d separations.) Neglect of the spin-orbit interaction will cause the biggest errors along the high-symmetry lines and planes which are the only places where more than one irreducible representation of the single group can occur.

The avoided crossings induced by the spin-orbit interaction may create new gaps, which in turn can, in principle, support surface states. In addition, the changed dispersion of the bands can alter the Fermi surface. For the spin-orbit interaction to have much of an effect, there must be degenerate states, and the spin-orbit coupling must be comparable to or larger than the crystal-field (including electron-hopping) effects. On transition-metals surfaces[14,15] such as W(110) and Mo(110), the effects of spin orbit on the d bands near the Fermi level (E_F) are significant since E_F falls near the $\Gamma_{25'}$ and Γ_{12} degenerate d states. For Ta, however, the Fermi level is below the $\Gamma_{25'}$ and Γ_{12} states. The d states of concern in Ta are singly degenerate, and thus the effects on the occupied states are correspondingly much smaller than for Mo or W. In Fig. 1 the scalar-relativistic (solid lines) and fully relativistic (dotted lines) bulk Ta bands along the Δ line (which projects down to $\bar{\Gamma}$

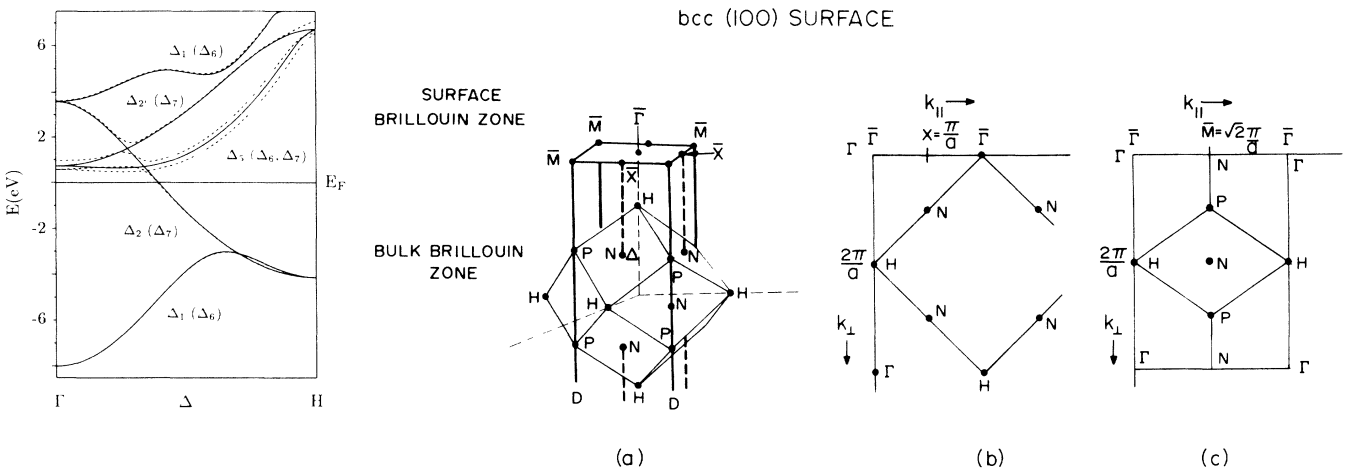

FIG. 1. Left: Bulk scalar-relativistic (solid lines) and fully relativistic (dashed lines) bands of Ta along $\Gamma \rightarrow H$. Right: bulk BZ of bcc structure and its projection onto the (001) surface BZ.

of the surface Brillouin zone) are shown. These self-consistent LDA bulk bands were calculated using the linearized augmented-Slater-type-orbital (LASTO) method.[16] Below the Fermi level, spin-orbit coupling has almost no effect on the dispersion of the bands. No gap is opened up where the bands cross since they belong to different double-group irreducible representations (Δ_6 and Δ_7) and thus can cross. Only similarly small spin-orbit-induced changes occur throughout the BZ, demonstrating that the spin-orbit interaction does not significantly alter the occupied LDA bands for the Ta(001) surface. (A possible exception will be discussed later.) Above the Fermi level, however, significant splittings and changes in the dispersion of the levels occur when the spin orbit interaction is included. Since for W and Mo the Fermi level falls near these states, the spin-orbit interaction will be more important in describing the occupied bands of these materials.

B. Surface relaxation and surface states

The presence of a surface is a large perturbation on the first few atomic layers. Since the local environment is different at bulk and surface sites, the first interlayer spacing of clean metal surfaces should differ in general from that of the ideal bulk-terminated solid. From simple bond-cutting/strength arguments, the naive expectation is that the surface layer should contract, and for most metal surfaces a small contraction is indeed observed. Since Ta has a large cohesive energy (8.1 eV/atom), the bond-strength arguments also suggest a rather substantial contraction due to the strengthening of the bonds between the surface and subsurface layers.

A LEED study[1] of the surface-layer relaxation of Ta(001) has previously reported a 10% contraction of the first interlayer spacing. Recently, a photoelectron-diffraction (PD) study,[12] employing the surface-shifted $4f$ core levels, has been performed. Comparing with multiple-scattering LEED-type calculations for Ta(001) surfaces with first interlayer contractions up to 15%, a 10% contraction of the surface was inferred. Note that neither the LEED nor PD determinations are direct measurements of the interlayer spacing. Total-energy calculations[11] for nine layer slabs of Ta(001) give a contraction of the first interlayer separation of $\sim 13.2\%$. The discrepancies between this theoretical value and previous values obtained from LEED and PD are within the experimental and theoretical uncertainties. The surface relaxation improves the agreement between theory[11] and experiment for the surface core-level shift. For the valence bands, there are also significant changes in the surface-state dispersions and positions accompanying the relaxation. The energy bands along $\bar{\Gamma}-\bar{X}-\bar{M}-\bar{\Gamma}$ in the surface BZ for Ta(001) are shown in Figs. 2(a) (bulk termination) and 2(b) (14% contraction of the first layer). All surface calculations reported here were done using the full-potential linear augmented-plane-wave (FLAPW) method.[17] States with a high percentage ($>60\%$) of their wave functions in the surface region are marked. Some of the particular changes are the following: (1) The unrelaxed slab has two resonances along both $\bar{\Delta}_2$ and $\bar{\Sigma}_2$ (the "2" label states odd with respect to the symmetry plane), while the relaxed slab has only one in each case. (2) The odd-symmetry states at $\bar{M}$ shift toward E_F by ~ 0.4 eV when the surface is relaxed. (3) The dispersion of the $\bar{\Sigma}_1$ and $\bar{\Delta}_1$ surface resonances near the Fermi level is modified. Because of the simpler structure of the odd-symmetry bands, it is easier to use the photoemission results for the $\bar{\Delta}_2$ and $\bar{\Sigma}_2$ resonances to choose between the ideal terminated and contracted-surface bands; from such a comparison, the photoemission results are in better agreement with the bands of the contracted surface [Fig. 2(b)]. Henceforth we will make comparisons to the bands corresponding to a 14% contraction of the first interlayer separation. We have not considered a reconstruction of the Ta(001) surface because there is no experimental evidence of a reconstruction and the $\bar{\Sigma}_2$ surface state that is believed responsible for the W(001) reconstruction is completely unoccupied.

Any direct comparisons of photoemission experiments and local-density calculations are subject to several

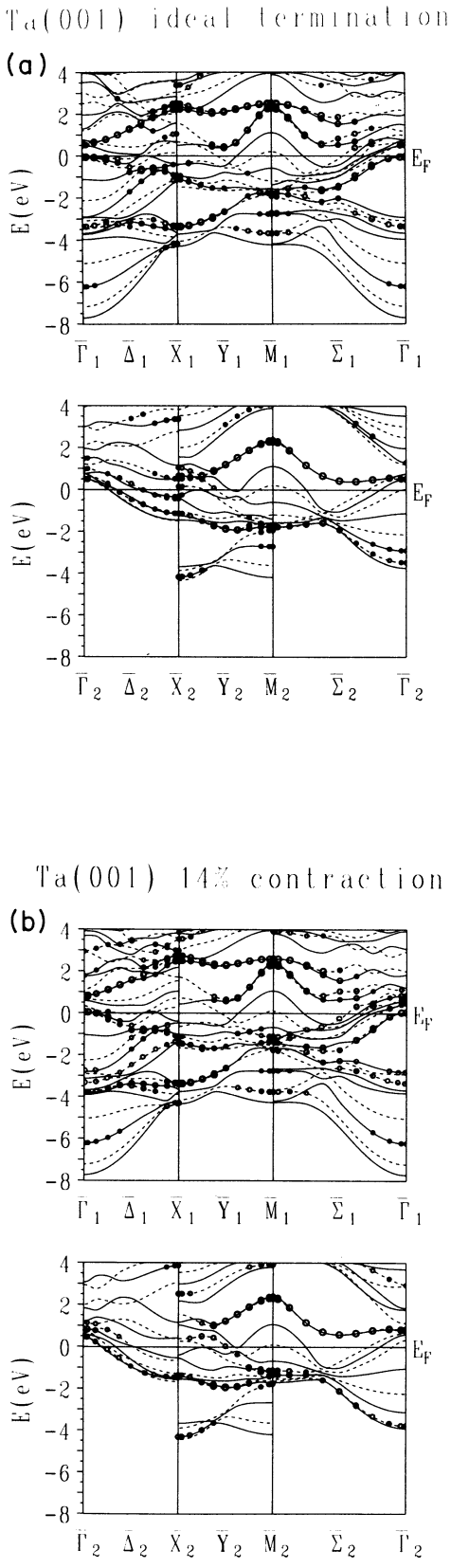

FIG. 2. Energy bands for nine-layer Ta(001) slabs for either (a) bulk terminated or (b) a 14% contraction of the first interlayer spacing, separated by mirror symmetry (top part, even; bottom, odd). States with at least 60% localization in the surface region are marked.

caveats. First and foremost, the local-density eigenvalues plotted are not quasiparticle energies that are measured; they are not even the true ground-state energies. However, if the valence hole created in the photoemission process is delocalized (the self-energy is small), then the eigenvalues are good approximations to the quasiparticle energies. Generally, one expects that materials near the beginning of the transition-metal series will be less correlated (the self-energy effects are smaller) and that the dispersion and position of states will be given approximately correctly by band calculations. While Ta(001) falls in this category, some differences between theory and experiment in regard to dispersions and positions of states are to be expected.

Another difficulty in comparing experiment and theory for surface calculations are finite-size effects. Most surface calculations (including the ones presented here) use a finite slab or supercell. In these methods the semi-infinite surface is approximated by a small number of layers. The reasonableness of this approximation rests on the short screening length and, even more importantly, on the fact that integral properties such as total energies and charge densities can be given accurately by finite samplings of reciprocal space. In the slab and supercell methods, the projected bulk band are given as a series of discrete slab bands: In an N-layer slab, each projected bulk band is represented by N bands. These slab bands, which must represent both bulk continuum and surface-resonance states, can be separated by on the order of an eV in energy. Thus, although the integral over all occupied states may be accurate, the calculated positions of individual resonances (which are not integral properties) will be dependent to some extent on the number of layers.

To get some measure of this effect, we also present the

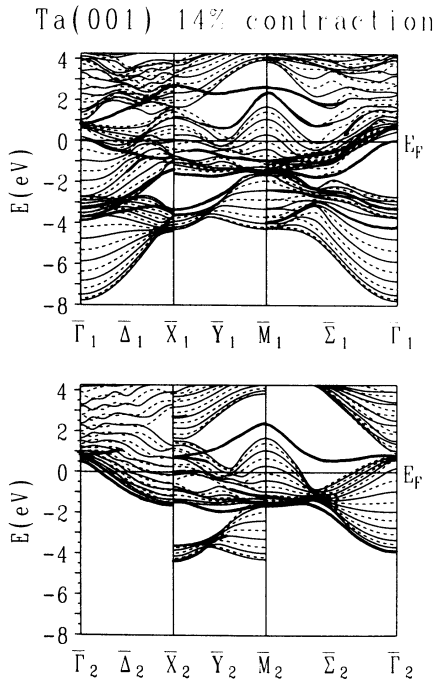

FIG. 3. Energy bands for a 21-layer Ta(001) slab with a 14% contraction of the first interlayer spacing for even (top) and odd (bottom) symmetry.

bands (Fig. 3) from a 21-layer Ta(001) film corresponding to a 14% contraction. These bands are obtained by a "stretching" method that uses the density and potential of the film and bulk to generate a thicker film. Although the results are not fully self-consistent, i.e., total energies are not completely converged, the bands are relatively stable. The dispersions and positions of the surface resonances are more obvious, as are the bulk symmetry-projected gaps. While the positions of the resonances are little changed, there are differences in the interpretation of some of the surface features. In particular, in the 21-layer films bands, the $\bar{\Sigma}_2$ and $\bar{\Delta}_2$ resonances are seen to be actually in the symmetry gaps, whereas from the nine-layer films they appeared to overlap the continuum. For the $\bar{\Delta}_1$ states, the main change is that the resonance that disperses down from $\bar{X}$ is now slightly deeper and closer to the projected band gap than in the nine-layer film.

The $\bar{\Sigma}_1$ resonances show the biggest changes in position and interpretation. The resonance at ~ 3 eV binding energy is now found to definitely overlap the continuum, and the surface state from $\bar{\Gamma}$ is clearly in the gap. The resonance that was seen to cross the Fermi level ~ 0.4 of the way from $\bar{\Gamma}$—$\bar{M}$ in the nine-layer film is better thought of as a surface-enhanced bulk feature: The bulk-band structure has some flat bands (in $k_\perp$) at these $\mathbf{k}_\parallel$. This grouping of states will show little dispersion with photon energy and thus mimic a surface resonance. (The center of these states crosses the Fermi level at ~ 0.43 Å^{-1}.) The calculations show more surface enhancement of the wave functions nearer to $\bar{M}$, which is also where the bulk bands become broader. Although the dispersion of this resonance near the Fermi level is mainly due to the bulk bands, this state may be further surface enhanced due to the spin-orbit coupling. Along $\bar{\Sigma}$, the spin-orbit coupling will destroy the remaining mirror symmetry and thus generate avoided crossings in the bulk bands. These avoided crossings induce additional critical points in the bands from which states can be split off. While this resonance can be understood without considering spin orbit, it seems likely that the spin-orbit interaction will tend to enhance the surface character of this resonance. Because of these various differences related to finite-size effects, our comparisons between theory and experiment use the resonances and bulk edges calculated for the 21-layer film.

Although there are a number of reasons why experiment and calculations should not agree, comparisons are still worthwhile. Discrepancies point out the limitations of the various theoretical approximations and some of the important physics beyond ground-state local-density calculations. On the other hand, the calculations provide important information about wave-function character, bonding, etc., which is difficult or impossible to extract from experiments alone, thus providing a more complete picture of the electronic structure of the surface.

IV. RESULTS AND DISCUSSION

A. Photoemission from the center of Brillouin zone

Normal-emission photoelectron spectroscopy was carried out for both *s*- and *p*-polarized light. Except for secondary backgrounds, no spectral feature was observed in the normal-emission angle-resolved photoemission spectra when using *s*-polarized light. A typical angle-resolved photoemission energy-distribution curve from Ta(001) is displayed in Fig. 4. The spectrum was created by 60°-incident *p*-polarized light with the polarization **A** vector in the plane of collection along $\bar{\Gamma} \rightarrow \bar{M}$. A sharp and intense feature near 0.2 eV is a surface-sensitive state in the valence band. A relatively broader feature at about 3 eV binding energy is actually composed of two surface-sensitive states that are located at 2.7 and 3.4 eV, respectively. These surface-sensitive features do not disperse in binding energy as a function of incident-photon energy, indicating that they are good candidates for the surface states of Ta(001). According to the theoretical calculations, there should be a Ta Δ_1 bulk band in a binding-energy range of 3–8 eV, which is not observable in this spectrum due to reasons that we will discuss later. Besides the valence-band features, there is a very broad bump centered at a binding energy of 12 eV. This is an Auger peak resulting from the relaxation of a pair of Ta valence electrons. One of the valence electron decays into the Ta $4f$ hole created by the direct photoelectron excitation; the other escapes into the continuum and is measured by the detector. Among the secondary-electron background, a broad feature located at about 23 eV binding energy is composed of four individual Ta $4f$ core levels. The $4f_{5/2}$ and $4f_{7/2}$ Ta bulk states are located at the binding energies of 23.6 and 21.7 eV, respectively. For each of these levels, the core states at the surface shift 0.75 eV to higher binding energy compared to the bulk levels due to the changed local environment at the surface. The spectra taken at larger photon energy show the well-separated peaks at binding energies of 21.7, 22.4, 23.6, and 24.3 eV, respectively. Finally, the work function of Ta(001) can be extracted from Fig. 4 by subtracting the width of the energy-distribution curve from the

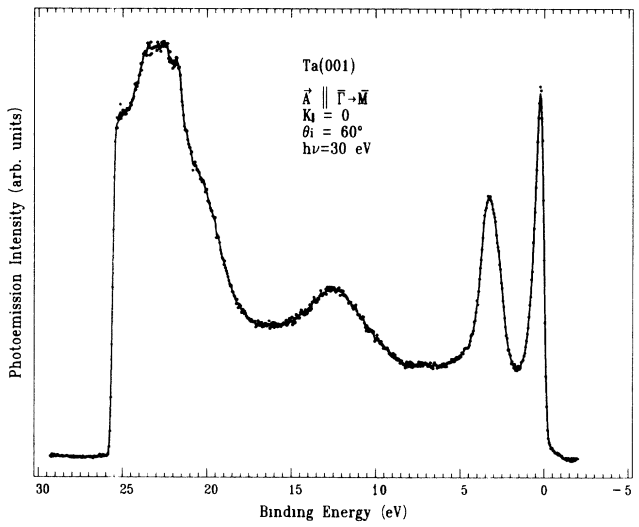

FIG. 4. Angle-resolved photoemission energy-distribution curve of Ta (001) taken by the 60°-incidence light and collected at the surface normal. The **A** vector of the polarized light is in the mirror plane of collection along $\bar{\Gamma} \rightarrow \bar{M}$.

incident-photon energy. A 4.1-eV work function is obtained in this normal-emission photoelectron spectroscopy measurement for Ta(001); the calculations give a value of 4.2 eV.

Since we are particularly interested in the surface electronic structure of Ta(001), the studies will mostly emphasize the valence-band energy region. Figure 5 shows a set of normal-emission photoelectron spectra taken at 45° incidence and various photon energies. A sharp feature appears at 0.2 eV below the Fermi level whose intensity varies as a function of incident-photon energy. This resonance was previously predicted in the calculation of Krakauer.[10] The asymmetry in the line shape near the Fermi level indicates that its center is located at or above the Fermi energy or else it is due to other mechanisms such as phonon broadening. With an instrumental resolution of 0.1–0.2 eV, it is difficult to pin down whether this surface resonance is centered above or below the Fermi level in the normal-emission spectra. One way

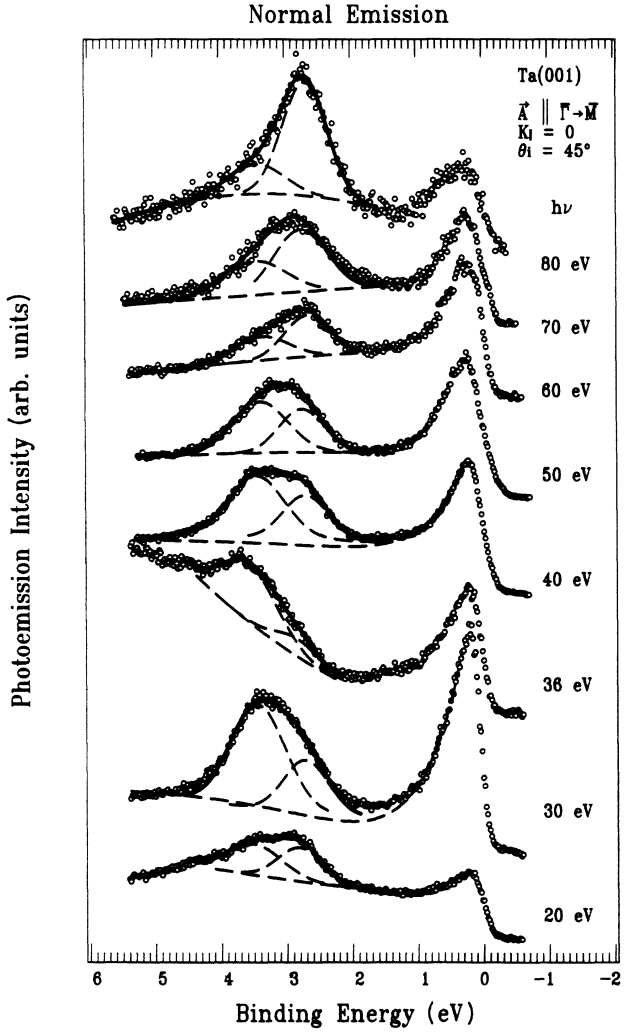

FIG. 5. Normal-emission photoelectron spectra from the Ta(001) surface taken at various photon energies and 45°-incidence angle. The polarization vector **A** was parallel to the $\bar{\Gamma}\rightarrow\bar{M}$ direction. The dashed curves are two Gaussian fits at a fixed FWHM of 0.34 and 0.42 eV.

to determine more precisely the position of the surface resonance near the Fermi level is to decompose its line shape with a Lorenzian and an instrumental broadening, and then compare these line shapes and widths with spectra taken at a $\mathbf{k}_{\parallel}$ where the resonance is below the Fermi level. In the Ta(001) case, unfortunately, the second surface resonance that crosses the Fermi level at about 0.4 Å^{-1} lies too close. This overlap prevents a "clean" measurement of the surface resonance and makes a determination of the full width at half maximum (FWHM) ambiguous.

In the inverse photoemission spectra, a surface state was observed at about 0.2 eV above the Fermi level at the $\bar{\Gamma}$ point. According to the band calculations for the 21-layer film of Ta(001), a surface resonance is predicted at the Fermi level (0.05 eV above E_F at $\bar{\Gamma}$). This indicates that the same surface-resonance state is being observed both above and below the Fermi level with two different experimental techniques. There are several related explanations. First, since the states are rather localized in space (as determined from the calculations), the self-energy differences between adding and subtracting an electron can account for the two results as long as the resonance extends both above and below E_F. A possible cause of this broadening of the surface resonance is the overlap with the $\bar{\Delta}_1$ symmetry continuum. The only bulk band that overlaps the totally even-symmetry surface resonance is a Δ_2 band, which has a different bulk symmetry, but as seen in Fig. 1, spin orbit will allow coupling of the resonance to the Δ_2 band. The signal-to-background ratio for the surface resonance in direct photoemission is significantly greater than that in inverse photoemission. As a first-order approximation, this suggests that the center of the surface resonance is located at the Fermi level, although such a conclusion is complicated by details of the experimental setup used in the inverse-photoemission experiments and the fact that bulk $\Gamma_{25'}$ transitions will contribute a larger background to the inverse-photoemission data.

The two features located at 2.7 and 3.4 eV are most clearly separated at 40 eV photon energy. Like the surface state at the Fermi level, the intensity of these states vary as a function of photon energy. In order to precisely determine any dispersion of these surface-sensitive states as a function of photon energy, curve fitting has been carried out on each spectrum. The structures at higher binding energy were fitted by two Gaussian peaks with fixed FWHM, but with variable binding energies and intensities. The values of the fixed FWHM of 0.24 and 0.42 eV for low and high binding energies of the surface states, respectively, were determined by fitting one of the best-resolved spectra with two Gaussian peaks. The binding energies of these two Gaussian peaks at 2.7 and 3.4 eV are found to hardly vary as a function of incident-photon energy from 14 to 100 eV.

To determine whether these surface states are in bulk gaps, great effort has been taken to attempt to identify the bulk bands of Ta(001). According to the band structure of Fig. 1, there are two bulk bands with symmetries Δ_1 and Δ_2 below the Fermi level and one of Δ_5 just above E_F that project to the $\bar{\Gamma}$ point of the Ta(001) surface BZ.

Since the final state of the electron is invariant under crystal operations for normal photoemission, the initial state must have the same symmetry as the dipole operator that causes the optical transition. In the case of Ta(001), only states with Δ_1 or Δ_5 symmetry can be excited in normal emission. Furthermore, initial Δ_1 states can be excited only by the normal component of **A** and the Δ_5 states only by the parallel component. Two results can be drawn from these selection rules. First, at $\bar{\Gamma}$ the resonances are derived from either Δ_5 bulk bands (the state near the Fermi level) or else from Δ_1 bands (the two resonances with greater binding energies). Second, a Ta bulk band with Δ_1 symmetry is expected to be seen in normal emission. We find that the spectra taken down to 15 eV below the Fermi level with various incident-photon energies show little trace if any of the Δ_1 band. Apparently, the cross section for the *sp* bulk states is small compared to the *d*-like surface resonances in our range of photon energies. (The Δ_1 state is predominantly *sp*-like near the bottom of the band.) Previous angle-resolved photoemission experiments[18] on Ta(001) using 70-eV *p*-polarized light did show a peak with small intensity at 6.7 eV binding energy. Besides the Δ_1 bulk band of Ta, oxygen and other hydrocarbons (*sp* states) are very sensitive to photon energy in this binding-energy region.

The number of surface-resonance states above the Fermi level remained an unsolved problem in the inverse-photoemission study. For the spectrum taken at normal incidence, the second feature located at 1 eV above the Fermi level was attributed to the bulk transition.[9] According to the LDA calculation for the 21-layer Ta(001) slabs, a surface resonance is predicted at an energy 0.8 eV above the Fermi level at $\bar{\Gamma}$. The dispersion of this surface resonance away from $\bar{\Gamma}$ along both $\bar{\Gamma}\rightarrow\bar{M}$ and $\bar{\Gamma}\rightarrow\bar{X}$ is confirmed by the inverse-photoemission results. Near $\bar{\Gamma}$, this state loses intensity compared to the bulk background. It should be noted that at $\bar{\Gamma}$, the bulk $\Gamma_{25'}$ levels are located at the same energy as the surface resonance. Besides the instrumental resolution, the overlap of the bulk $\Gamma_{25'}$ levels with the surface resonance at 0.8 eV

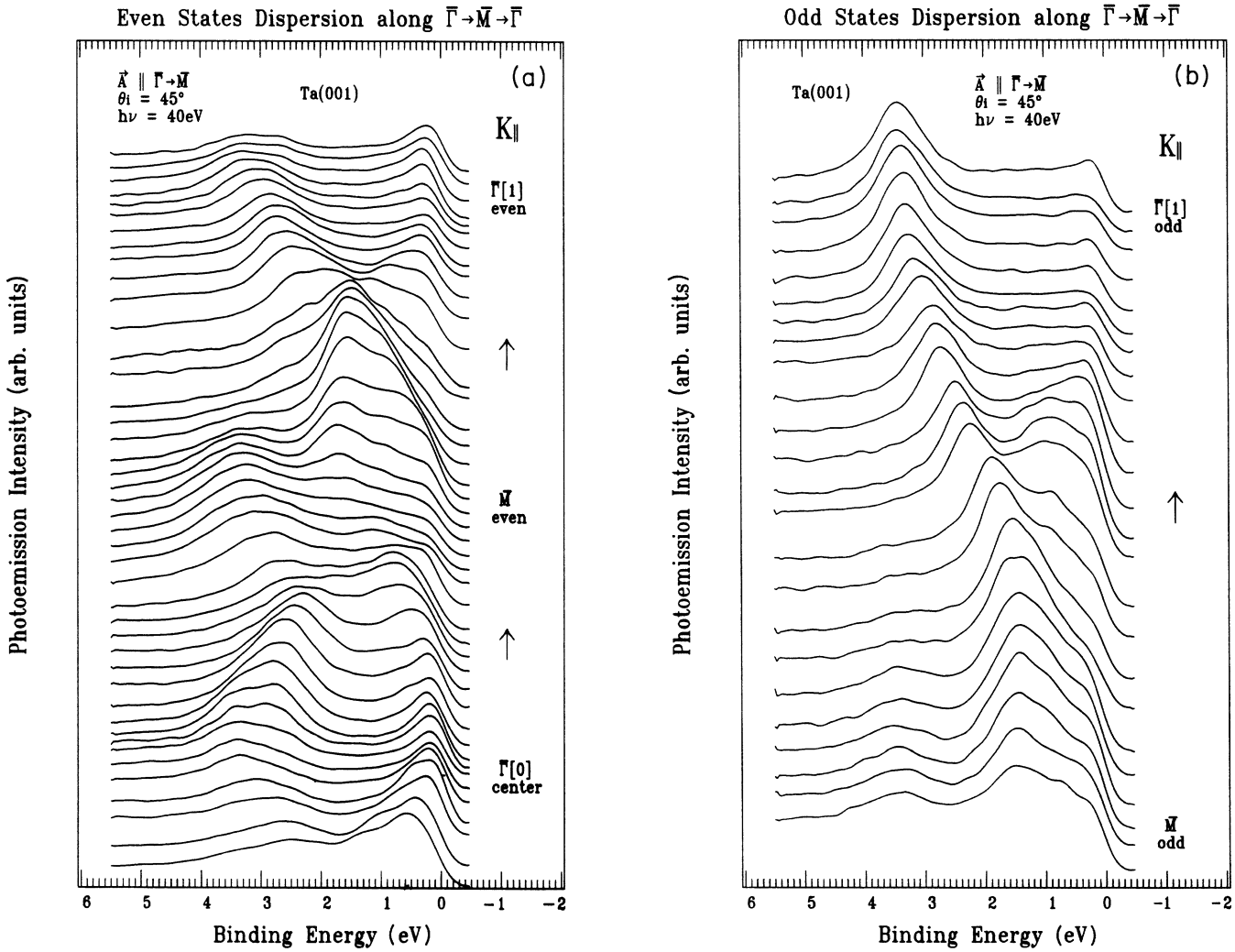

FIG. 6. Angle-resolved photoelectron spectra from Ta(001) taken at various azimuth angles along the $\bar{\Sigma}$ direction. The photon energy was 40 eV and the angle of incidence was 45°. The polarization vector **A** is (a) in the mirror plane of collection or (b) perpendicular to the mirror plane of collection.

above the Fermi level may have prevented the experimental identification of this surface resonance in the previous inverse-photoemission study.[9] In addition, and perhaps more importantly, spin-orbit effects will be significant for the unoccupied states near $\bar{\Gamma}$ probed by the IPE experiments, with the possible result that the states near $\bar{\Gamma}$ are more strongly coupled to the bulk states than the SRA calculations would suggest.

B. Dispersion along $\bar{\Gamma} \rightarrow \bar{M}$

The surface-state dispersion along $\bar{\Gamma} \rightarrow \bar{M}$ is especially interesting because the surface atomic displacements of the $c(2\times2)$ reconstruction of W(001) is along this direction. Angle-resolved photoemission measurements[8] for W(001) show that a $\bar{\Sigma}_2$ surface state crosses the Fermi level at about halfway toward $\bar{M}$. It is generally believed that this state is responsible for the observed reconstruction. A careful examination of the surface resonances of Ta(001) along the same direction will give us further insight into these types of transition-metal surface reconstructions.

Photoemission spectra obtained along $\bar{\Gamma} \rightarrow \bar{M}$ of the Ta(001) surface BZ are shown in Fig. 6(a) for even symmetry and in Fig. 6(b) for odd symmetry. In the even-symmetry configuration, only $\bar{\Sigma}_1$ symmetry states will be excited by p-polarized light with the polarization vector **A** along $\bar{\Gamma}-\bar{M}$. The d-electronic states that have $\bar{\Sigma}_1$ symmetry are d_{z^2}, d_{xy}, and $d_{(x+y)z}$ orbitals. As shown in Fig. 6(a), when the emission angle increases along the even-symmetry direction, the sharp feature at the Fermi level disperses downward, reaching the $\bar{M}$ point at 1.8 eV binding energy. A second feature crosses the Fermi level at about 0.4 Å^{-1} and reaches its maximum binding energy at 1.0 Å^{-1}. As discussed above, the surface localization of this state may be enhanced due to the spin-orbit coupling. The low-lying surface resonance at 2.7 eV disperses upwards and reaches its minimum binding at $\bar{M}$, with the same energy at $\bar{M}$ as the peak that disperses downward from the Fermi level. The high-lying surface-resonance state at 3.4 eV binding energy shows a symmetry around the half of the surface BZ with a minimum binding at about 2.5 eV at 0.55 Å^{-1}. The odd-symmetry photoemission spectra were obtained by setting the polarization vector **A** of the s-polarized light perpendicular to the mirror plane of collection. In this case, only the initial states with $\bar{\Sigma}_2$ symmetry (such as $d_{x^2-y^2}$ and $d_{(x-y)z}$ orbitals) will be excited and detected along $\bar{\Gamma} \rightarrow \bar{M}$. The electronic structure is very simple for this symmetry. Only a single surface resonance is predicted by the 14% contracted film. The spectra taken for odd symmetry along $\bar{\Gamma} \rightarrow \bar{M}$ are excited by the s-polarized light with polarization vector **A** perpendicular to the mirror plane of collection. The spectra in Fig. 6(b) show a much clearer picture of the odd-state dispersion. At this setting, only one surface-resonance state appears and disperses from 3.4 eV binding energy at the zone center upwards to 1.4 eV at the $\bar{M}$ point. The FWHM of this surface resonance is determined to be about 0.7 eV.

Figure 7 plots the dispersion of the surface-sensitive features as a function of $\mathbf{k}_\parallel$ along $\bar{\Sigma}$ with even (top) and odd (bottom) symmetry. The circles are angle-resolved photoemission results from Figs. 6(a) and 6(b). The squares are the inverse-photoemission results from Ref. 9. The solid lines are the predicted surface resonances from the self-consistent calculations for the 9- and 21-layer 14% contracted Ta(001) slabs. The shaded regions are the projections of the bulk bands of either even or odd symmetry. For $\bar{\Sigma}_1$ symmetry, which has even reflection with respect to the plane that contains the surface normal and the $\bar{\Gamma} \rightarrow \bar{M}$ direction, the $\bar{\Gamma}$ resonance at E_F is in the symmetry gap for the 21-layer film. This indicates a weak coupling of the surface resonance with the bulk band. Consistent with this picture, the contamination tests show that the states at 0.0 and 2.7 eV are more surface sensitive than the surface resonance in the projected bulk-band region. The surface resonance at 3.4 eV at $\bar{\Gamma}$ is complicated by two facts. First, this state has both an even ($\bar{\Sigma}_1$) and odd ($\bar{\Sigma}_2$) surface resonance away from $\bar{\Gamma}$. Second, for even symmetry, this state is located in the projected bulk-band region; i.e., this state can couple more strongly with the bulk bands and decay further into the near-surface region. The local-density calculation for

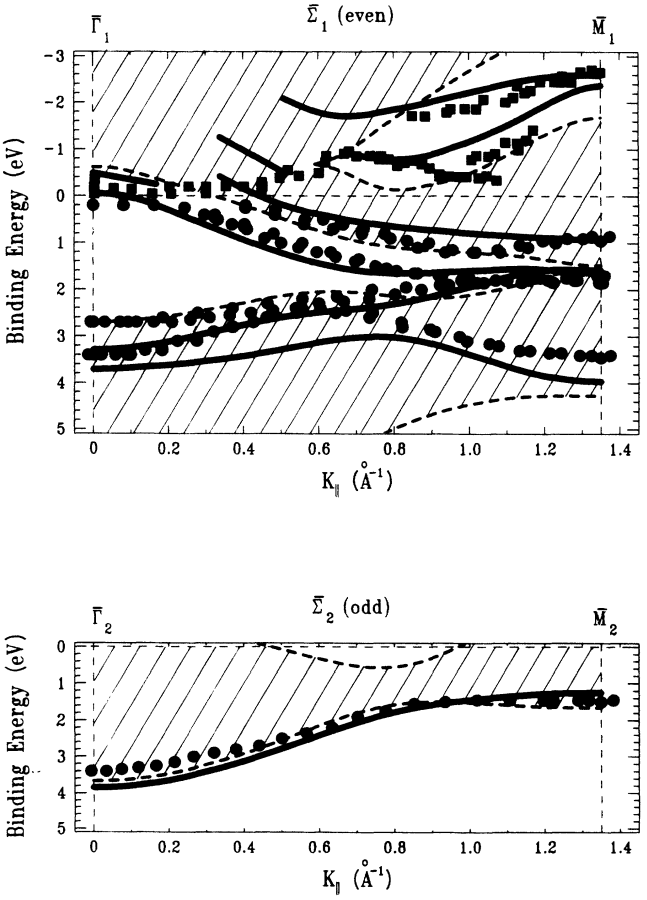

FIG. 7. Dispersion of surface resonance states on Ta(001) along $\bar{\Sigma}$. Circles are experimental results, squares are the IPE results of Ref. 9, the slanted lines represent the projected bulk bands, and the solid lines are the predicted resonances from a 14% contracted Ta(001) film.

the 21-layer Ta(001) slab shown in Fig. 3 gives detailed information on the wave-function character of the surface resonances. Comparing them with the experimental data in Fig. 7, the d characters of these surface resonances can be identified. For example, three even-symmetry d orbitals, d_{z^2}, d_{xy}, and $d_{(x+y)z}$, may exist along the $\bar{\Gamma}\rightarrow\bar{M}$ direction. Each surface state may be a combination of the three orbitals throughout the surface BZ. The LDA calculation indicates that the three surface resonances below the Fermi level are mainly d_{z^2} in character. Above the Fermi level, the first $\bar{\Sigma}_1$ resonance is composed of both d_{xy} and $d_{(x+y)z}$ orbitals, and the one with the highest energy shown in Fig. 7 is mainly d_{xy}. Calculations also show that the resonance that crosses the Fermi level at about 0.4 Å^{-1} is relatively less surface sensitive than the rest of the surface resonances. Unlike the case of W(001), in which a surface resonance in a bulk gap crosses the Fermi level at about halfway along $\bar{\Gamma}\rightarrow\bar{M}$, the strong coupling of this surface resonance with the bulk band makes the Ta(001) surface relatively more stable. For the odd-symmetry case, the calculation indicates that the only surface resonance below the Fermi level is mostly $d_{x^2-y^2}$ in character.

In Fig. 7, we also compare the previous inverse-photoemission results[9] with the local-density calculations. Since in the IPE experiments, no determination of the symmetry of the electronic states is possible without photon-polarization information, all the IPE data are plotted in the $\bar{\Sigma}_1$ portion of Fig. 7. (For the predicted $\bar{\Sigma}_2$ resonance, see Fig. 3.) Two distinct surface resonances are predicted above the Fermi level in the symmetry gap along $\bar{\Gamma}\rightarrow\bar{M}$ direction. The experimental data agree rather well in the symmetry gap with the theoretical calculation. Near the midpoint of the surface BZ, the $\bar{\Sigma}_1$ and $\bar{\Sigma}_2$ resonances separate, with the $\bar{\Sigma}_1$ resonance theoretically losing intensity as it crosses the bulk continuum. The $\bar{\Sigma}_2$ resonance is predicted to remain localized to the surface throughout the zone. Note that this is the resonance that crosses the Fermi level in the case of W(001). The IPE measurements show that the peak near the Fermi level at normal incidence does not disperse appreciably until about halfway to the surface-BZ edge. If this peak is due to the broadening of the surface resonance at the Fermi level, most of the discrepancies can be

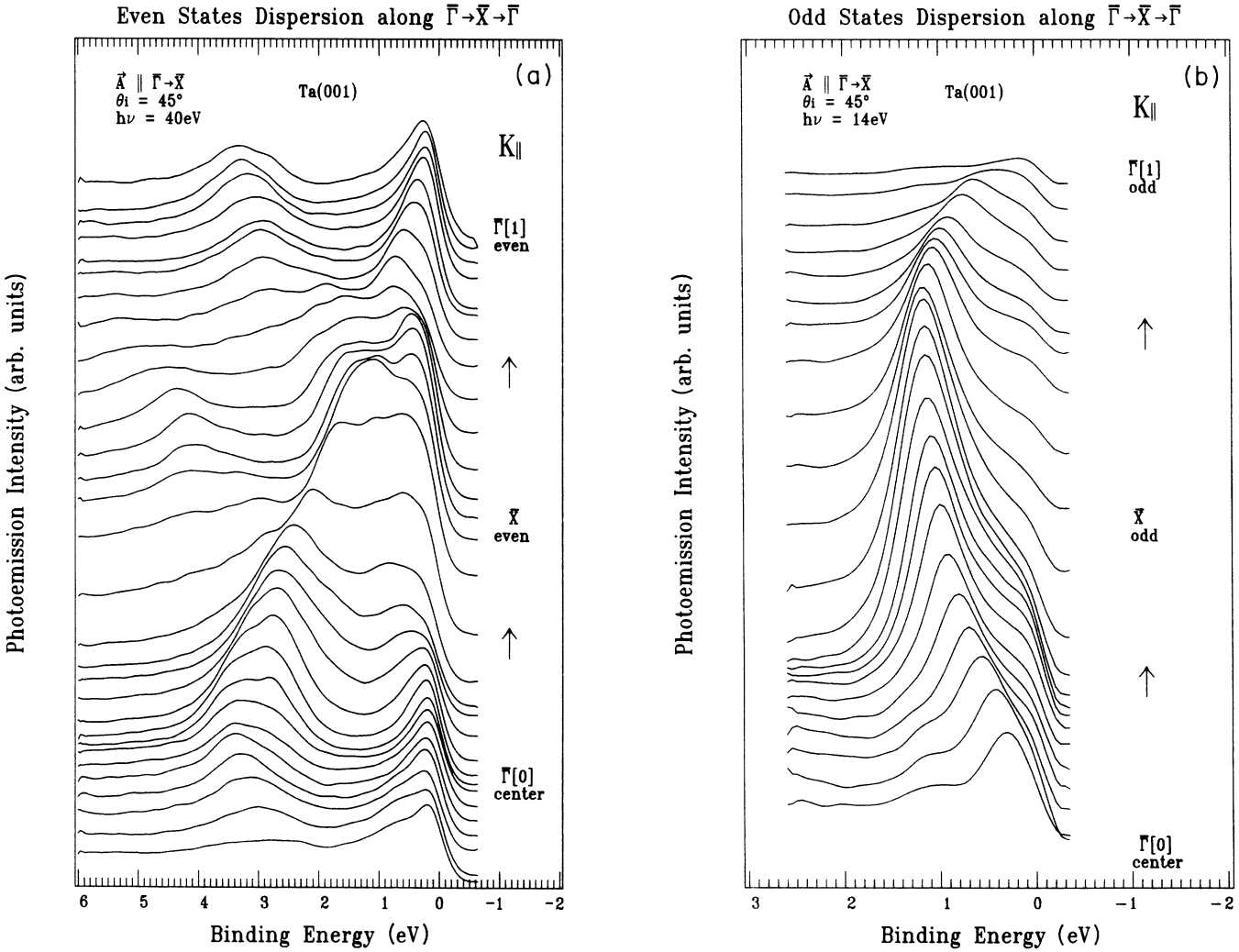

FIG. 8. Angle-resolved photoelectron spectra for the (a) even and (b) odd states of Ta(001) taken at various polar angles along the $\bar{\Delta}$ direction. The photon energy was 40 eV and the angle of incidence was 45°.

resolved because the dispersion of the d surface resonance below the Fermi level is quite flat. Besides the contribution of the occupied surface resonance near $\bar{\Gamma}$, the surface resonance that crosses the Fermi level at 0.4 Å^{-1} will have a direct effect on the peak observed in the inverse-photoemission experiments.

C. Dispersion along $\bar{\Gamma} \rightarrow \bar{X}$

Photoemission spectra obtained for even symmetry along the $\bar{\Gamma} \rightarrow \bar{X}$ azimuth of the Ta(001) surface BZ are shown in Fig. 8(a). As was mentioned before, to obtain the pure even symmetry, the angle-resolved system is set up in such a way that the polarization **A** vector of the p-polarized light is in the mirror plane of collection along $\bar{\Gamma} \rightarrow \bar{X}$. In this configuration, the spectra will probe only initial states that have $\bar{\Delta}_1$ symmetry, such as d_{z^2}, $d_{x^2-y^2}$, and d_{xz} orbitals. As shown in Fig. 8(a), the surface resonance at the Fermi level for the normal-emission spectrum is observed to disperse downwards as the emission angle increases. The dispersion of this state is relatively flat compared to its dispersion along $\bar{\Sigma}$. Two surface-sensitive states move up toward the Fermi level. At about half of the zone length, these two states split. The lower-binding-energy surface-sensitive state continues to disperse upwards and reaches a minimum at the $\bar{X}$ point. The deeper state disperses downwards. Its intensity is reduced significantly, making it very difficult to identify its position at $\bar{X}$. Besides the low intensity of the state at $\bar{X}$, the overlap of the three surface-sensitive states around $\bar{X}$ makes peak-position identification difficult. To estimate the binding energies of these states at the $\bar{X}$ point, the energy-distribution curves are fitted by three Gaussian-function line-shape peaks with binding energies of 0.18, 0.95, and 1.25 eV, respectively. The dispersion of these states around $\bar{X}$ is determined when comparing several sets of data in the first and second zones along the $\bar{\Gamma} \rightarrow \bar{X}$ direction. The angle-resolved photoemission spectra taken along the $\bar{\Gamma} \rightarrow \bar{X}$ direction with odd symmetry are shown in Fig. 8(b). The spectra were excited by the s-polarized light and collected by the angle-resolved detector along the mirror plane that is perpendicular to the **A** vector. The initial states appearing in these spectra will be of $\bar{\Delta}_2$ symmetry. They can be either d_{xy} or d_{yz} orbitals. Figure 8(b) shows a single peak dispersing from near the Fermi level to its maximum in both binding energy and intensity at the $\bar{X}$ point. This state is sensitive to contamination and hydrogen chemisorption. The LDA calculations show that it is a surface resonance located in the symmetry gap throughout the whole surface BZ.

We plot the dispersion of the surface-sensitive features from Fig. 8(a) with respect to $k_{\parallel}$ in the top portion of Fig. 9 for even symmetry, along with the results of the LDA calculations. As previously, the solid curves are the predicted surface resonances, the crosshatched regions are the projected bulk bands from the LDA calculation, the circles are the angle-resolved photoemission data from the Fig. 8(a), and the squares are the inverse-photoemission data from Ref. 9. The surface resonance near the Fermi level follows rather well the theoretical predictions. It is likely that this is the same surface resonance, with its tail broadened above the Fermi level, observed in the inverse-photoemission spectra along the $\bar{\Gamma} \rightarrow \bar{X}$ dispersion. The other two surface resonances have a similar dispersion trend as that along the $\bar{\Gamma} \rightarrow \bar{M}$ direction. For even symmetry, the agreement for the binding-energy position of the surface resonances is not as good as that along $\bar{\Gamma} \rightarrow \bar{M}$, partly due to the greater coupling into the bulk bands and the lack of even-symmetry band gaps along this direction. The inverse-photoemission results are traced rather well by the LDA calculation near the $\bar{X}$ point. Around the zone center, the surface resonance is predicted to disperse through the even-symmetry gap. From continuity of the wave function with wave vector, a surface resonance should not disappear inside the gap. The apparent disappearance of the resonance in the IPE results[9] may be due to experimental difficulties in separating the resonance from the background due to the bulk $\Gamma_{25'}$ transitions and/or the effects of spin orbit on the unoccupied states.

As in the case along $\bar{\Gamma} \rightarrow \bar{M}$, the angle-resolved photoemission spectra along $\bar{\Gamma} \rightarrow \bar{X}$ for odd symmetry [Fig. 8(b)] is much simpler and the dispersion of the surface state is also much more straightforward. The high intensity of the surface state in a featureless background makes it possible to determine the dispersion of this state

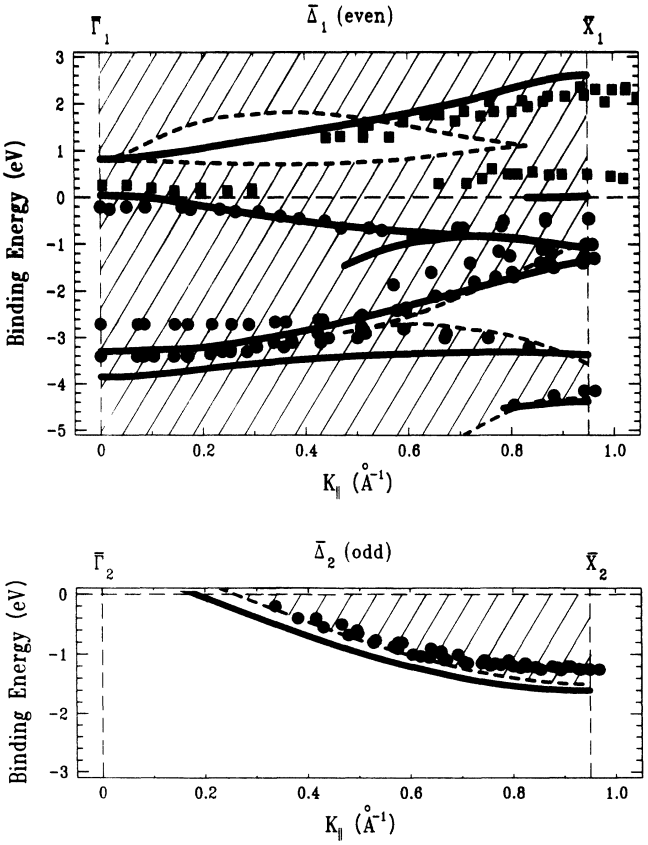

FIG. 9. Dispersion of the surface resonance states on Ta(001) along $\bar{\Delta}$. Circles are experimental results, squares are the IPE results of Ref. 9, the slanted lines represent the projected bulk bands, and the solid lines are the predicted resonances for a 14% contracted Ta(001) film.

precisely. Figure 8(b) shows the angle-resolved photoemission spectra taken along the $\bar{\Gamma}\rightarrow\bar{X}$ using 45°-incidence 40-eV photons. A well-defined surface resonance is observed to cross the Fermi level at 0.32 Å^{-1} and disperses downwards, reaching its minimum at a binding energy of 1.2 eV at $\bar{X}$. The intensity of the peak grows significantly as it moves away from the Fermi level, increasing in intensity by a factor of 5 near the $\bar{X}$ point. The FWHM of this surface resonance is determined to be 0.7 eV, an indication that its wave function is rather localized to the surface.

The bottom part of Fig. 9 compares the experimental results with the theoretical calculations for the bulk-band edges and the surface resonance with odd symmetry along $\bar{\Delta}$. The meaning of the symbols are the same as for the even symmetry. The dispersion trend from the experiment agrees rather well with the theoretical prediction that the surface resonance will follow the bottom edge of the Ta bulk band. The calculations show that this surface resonance is located in the symmetry gap with very little coupling to the bulk bands. That the surface resonance crosses the Fermi level in a symmetry gap might lead one to think that the Ta surface atom is unstable along the $\bar{\Gamma}\rightarrow\bar{X}$ direction, similar to the case of W. As will be discussed, this is not true.

All these surface resonances appear to disperse throughout the entire surface BZ, following the edge of the bulk bands from which they are derived. The significant d character of these surface resonances corresponds rather well to the dispersion of local-density calculations. However, there is a disagreement between the experimental data and LDA calculation in the absolute binding energies of surface resonances (and bulk-band edges) that are away from the Fermi level. Angle-resolved photoemission experiment data show that the two low-lying surface resonances are located at 2.7 and 3.4 eV below the Fermi level at $\bar{\Gamma}$. The LDA calculations for the 21-layer Ta(001) slab with a 14% surface-layer contraction predict two surface resonances at $\bar{\Gamma}$ with binding energies of 3.3 and 3.8 eV, respectively. Similar disagreement on the absolute binding energy of surface resonance is observed for odd symmetry along $\bar{\Gamma}\rightarrow\bar{M}$. The experimental surface resonances are consistently 0.3 eV lower in binding energy than the LDA results. Furthermore, the inverse-photoemission results indicate that the surface resonance reaches $\bar{X}$ at 2.3 eV above the Fermi level, whereas the LDA calculations place the resonance at 2.6 eV at $\bar{X}$. The disagreements seem to become larger for the surface resonances that are located farther away from the Fermi level. These discrepancies are much larger than the instrumental resolution of either the angle-resolved photoemission or the inverse-photoemission experiments. The differences are most likely related to errors in the LDA and to the neglect of self-energy effects, i.e., comparing a ground-state calculation to the excited-state quasiparticle spectrum probed by photoemission.

D. Polarization effects

Our normal-emission angle-resolved photoelectron spectra taken with s- and p-polarized incident light indicate that all three surface resonance of Ta(001) at $\bar{\Gamma}$ can only be detected when excited by p-polarized light. At near-normal-emission configuration, no spectral feature is observed when using s-polarized light. This suggests that the surface resonances are of even symmetry with respect to the Δ along the surface-normal direction. We took advantage of this to determine the Δ_2 bulk band along the surface normal. With the significant reduction in the intensity of the surface resonances when excited by the s-polarized light, one would expect to see the Δ_2 bulk-band dispersion as a function of photon energy. In our experiments, no photon-energy-dependent states were observed in the binding-energy range of 6 eV below the Fermi level. It is possible that the cross section of Δ_2 bulk band is small because it is mostly composed of sp-electron orbitals.

The character of the wave functions of the surface features at $\bar{\Gamma}$ can be determined from the symmetry decomposition given in Figs. 7 and 9. The surface resonances at 0.0 and 2.7 eV binding energy have symmetries $\bar{\Delta}_1$ and $\bar{\Sigma}_1$, while the one at 3.4 eV has $\bar{\Delta}_1$ and $\bar{\Sigma}_1, \bar{\Sigma}_2$ symmetries. The d-wave-function characters consistent with $\bar{\Delta}_1$ are d_{z^2}, $d_{x^2-y^2}$, and d_{xz}. The $\bar{\Sigma}_1$ states have d_{z^2}, $d_{(x+y)z}$, and d_{xy} character, while $\bar{\Sigma}_2$ states are either $d_{(x-y)z}$ or $d_{x^2-y^2}$. Thus the states at E_F and 2.7 eV are of d_{z^2} character. The d_{xz} character can be ruled out since d_{xz} and d_{yz} must be degenerate and no $\bar{\Delta}_2$ states exist in that energy range. The state at 3.4 eV has both $\bar{\Sigma}_1$ and $\bar{\Sigma}_2$ symmetry and thus must contain both d_{z^2} and $d_{x^2-y^2}$ orbitals. These conclusions can be tested using the polarization dependence of the states at point $\bar{\Gamma}$ in the surface BZ.

The polarization dependence of the electronic state has been calculated by Weng *et al.*[7] By considering the macroscopic effects of reflection and refraction in the classical electromagnetic formula, they found that the dependence of the two components of the $\mathbf{A}$ vector along the surface normal and along the sample surface is significantly different as a function of the incident angles. The magnitude of $\mathbf{A}_{\parallel}$ decays monotonically from 0° to 90° as a function of incidence angle. The magnitude of $\mathbf{A}_{\perp}$ shows a maximum at 50° incidence. Comparing the photoemission intensity of the surface resonance with their calculation, the component of $\mathbf{A}$ that plays a major role in the photoelectron-excitation process can be determined. Hence the wave-function character of the surface resonance at that specific $k_{\parallel}$ point can be obtained. The polarization dependence of the surface resonances from the angle-resolved photoemission is shown in Fig. 10. The photoemission intensity of all three surface resonances increases as the photon angle of incidence increases away from the surface normal. The maximum intensity is observed at about 50° angle of incidence. This suggest that at $\bar{\Gamma}$ all three surface resonances can be excited by the $\mathbf{A}_{\perp}$ component. In other words, at $\bar{\Gamma}$ all three surface resonances have dominantly $\bar{\Delta}_1$ symmetry.

Three d-electronic orbitals on Ta(001) have $\bar{\Delta}_1$ symmetry. They are d_{z^2}, $d_{x^2-y^2}$, and d_{xz} orbitals. Another way to determine precisely the wave-function characters from the experiment is to combine the polarization property of

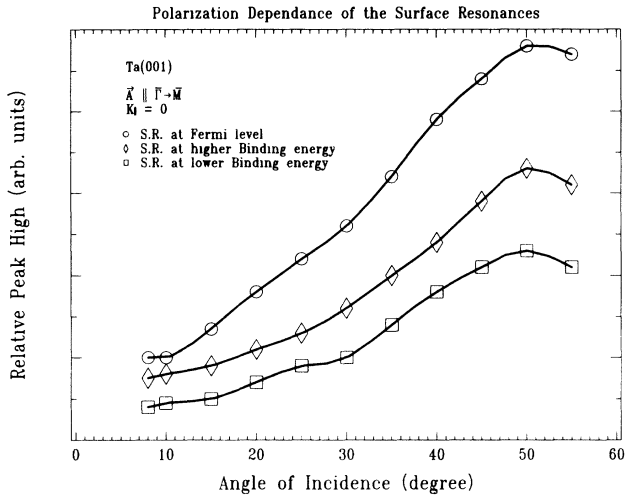

FIG. 10. Photoemission intensity of three surface resonances of Ta(001) at normal exit plotted as a function of the angle of incidence of the *p*-polarized light. The angle of incidence is the same as the angle of the photons polarization **A** and the sample surface $\bar{\Gamma}\rightarrow\bar{M}$ direction.

the synchrotron-radiation light with the final-state effect in the angle-resolved photoelectron spectroscopy. The independent rotation of the sample and detector allows one to pin down the even or odd symmetry of the initial electronic states with respect to the collection plane. Figure 11 compares the normal-emission spectrum taken from the zone center with three spectra from the second zone centers in the surface BZ. The normal-emission spectrum taken from the surface-BZ center labeled by $\Gamma[0]$ contains three peaks at 0.0, 2.7 and 3.4 eV binding energies, respectively. States appearing at normal emission indicate $\bar{\Delta}_1$ and $\bar{\Sigma}_1$ symmetry, but they may still contain both even- and odd-symmetry *d* orbitals with respect to the $\bar{\Gamma}\rightarrow\bar{M}$ and $\bar{\Gamma}\rightarrow\bar{X}$ directions. The spectrum labeled by $\Gamma[1]_{\text{even}}$ was taken from the second surface-BZ center along $\bar{\Gamma}\rightarrow\bar{X}$ with **A** parallel to the collection plane. Only those $\bar{\Delta}_1$ states that have even symmetry with respect to $\bar{\Gamma}\rightarrow\bar{X}$ will be observed, such as d_{z^2}, $d_{x^2-y^2}$, and d_{xz} orbitals. All three surface resonances observed at the normal-emission spectrum can be identified at this spectrum. Now let us take a look at the spectra taken from the second surface BZ along the $\bar{\Gamma}\rightarrow\bar{M}$ direction. The spectrum designated with $\Gamma[2]_{\text{even}}$ has **A** in parallel to the collection plane. This time only those $\bar{\Sigma}_1$ states that have even symmetry with respect to $\bar{\Gamma}\rightarrow\bar{X}$ will be observed. They are d_{z^2}, d_{xy}, and $d_{(x+y)z}$ orbitals. Three surface resonances appear at 0.0, 2.7, and 3.4 eV below the Fermi level. Note that only d_{z^2} orbitals can be excited and detected in all three configuration labeled by $\Gamma[0]$, $\Gamma[1]_{\text{even}}$, and $\Gamma[2]_{\text{even}}$. The spectrum taken for the pure odd symmetry adds some interesting results. The spectrum designated $\Gamma[2]_{\text{odd}}$ was taken in the second zone center along $\bar{\Gamma}\rightarrow\bar{M}$ with **A** perpendicular to the collection plane. In this configuration, only odd-symmetry initial states with respect to the $\bar{\Gamma}\rightarrow\bar{M}$ will be excited and detected in the photoelectron spectroscopy. These are $d_{x^2-y^2}$ and $d_{(x-y)z}$ orbitals. The photoemission spectrum shows only one peak at 3.4 eV below the Fermi level. The surface resonance at 3.4 eV binding energy appears in both the spectra for even symmetry along $\bar{\Gamma}\rightarrow\bar{X}$ and for odd symmetry along $\bar{\Gamma}\rightarrow\bar{M}$. The only *d*-electronic state that can disperse throughout these two symmetry surface BZ's is a $d_{x^2-y^2}$ orbital. The surface resonances observed at E_F and at a binding energy of 2.7 eV at the $\bar{\Gamma}$ point are mostly d_{z^2} orbitals. The surface resonance at 3.4 eV binding energy is composed of both d_{z^2} and $d_{x^2-y^2}$ orbitals. By use of polarization effects in the photoemission experiments, it is possible to determine the wave-function character of the $\bar{\Gamma}$ resonances purely from experiment. These assignments are consistent with the calculations for Ta(001).

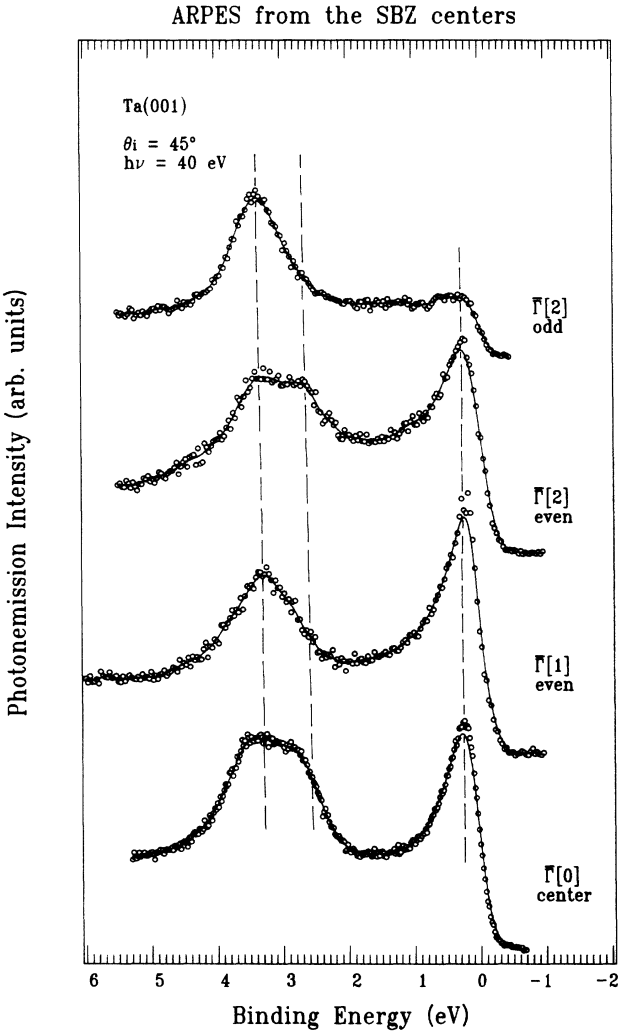

FIG. 11. Photoelectron-energy distributions for Ta(001) at various BZ centers. (a) zone center, (b) second zone center along $\bar{\Gamma}\rightarrow\bar{M}$ with even symmetry, (c) second zone center along $\bar{\Gamma}\rightarrow\bar{X}$ with even symmetry, and (d) second zone center along $\bar{\Gamma}\rightarrow\bar{M}$ with odd symmetry.

E. Spin-orbit interaction

In many cases, the inclusion of the spin-orbit interaction in a nonrelativistic or a scalar-relativistic calculation can create a new band gap or fill an existing gap by altering the bulk-band continuum. Recently, it has been shown that relativistic effects play an important role in the surface electronic of transition metals such as Ta, W, and Mo. Introducing spin orbit in an otherwise nonrelativistic tight-binding Hamiltonian, Treglia *et al.*[19] found improved agreement between the experimental and theoretical surface core-level shifts for Ta(001) and W(001). Mattheiss and Hamann[20] have shown that the addition of spin-orbit coupling modifies the dispersion of the scalar-relativistic surface-state bands and provides a slightly better agreement with the angle-resolved photoemission data for W(001). For W(110) and Mo(110), Gaylord and co-workers[14,15] have observed several surface resonances in a pseudogap opened by spin-orbit-induced hybridization.

From the bulk calculations with and without spin orbit (Fig. 1), we see that for Ta the bands that have been significantly modified by the spin-orbit coupling are unoccupied, whereas for W these states are near the Fermi level. While the spin-orbit interaction does create additional splittings and gaps for Ta above the Fermi level, the bands below the Fermi level are perturbed very little by the spin-orbit interaction, although the other relativistic effects included in the SRA have a significant effect on the bands. The existence and dispersion of the experimentally observed resonances are well described by the scalar-relativistic bands, implying that the spin-orbit coupling term is not required to interpret the occupied band structure of Ta(001), with the possible exception (as discussed above) of the surface enhancement of the $\bar{\Sigma}_1$ bulk bands and resonance that cross the Fermi level at about 0.4 Å^{-1}.

F. Surface-layer relaxation

The solid-vacuum interface breaks the translational symmetry of the system. Because of the resulting changes in the local environment of the surface atoms, the positions of the surface atoms are in general different from the ideal bulk termination. Comparing the Ta(001) bands for the bulk-terminated surface [Fig. 2(a)] and for the 14% contracted-surface layer [Fig. 2(b)] with each other and with experiment, there are noticeable differences. The differences are most obvious for the odd-symmetry dispersions. For example, the bulk-terminated bands predict two $\bar{\Delta}_2$ and two $\bar{M}_2$ surface-sensitive states, separated by about 1 eV. The experimental results for the odd-symmetry configuration, shown in Figs. 6 and 8, show only a single state along these two directions. The open circles are the experimental data, with the diameter of the circle approximately equal to the instrumental error bar. The position and dispersions of the resonances are well reproduced by the 14% contracted calculation, whereas the bulk-terminated surface has significant errors in the number and position of resonances. Hence inclusion of surface relaxation is necessary for the band-structure calculations to successfully describe the experimentally derived surface electronic structure of Ta(001). While a precise determination of the surface contraction is not possible by comparing experimental and calculated bands, such a comparison can help place limits. In the present case, the photoemission

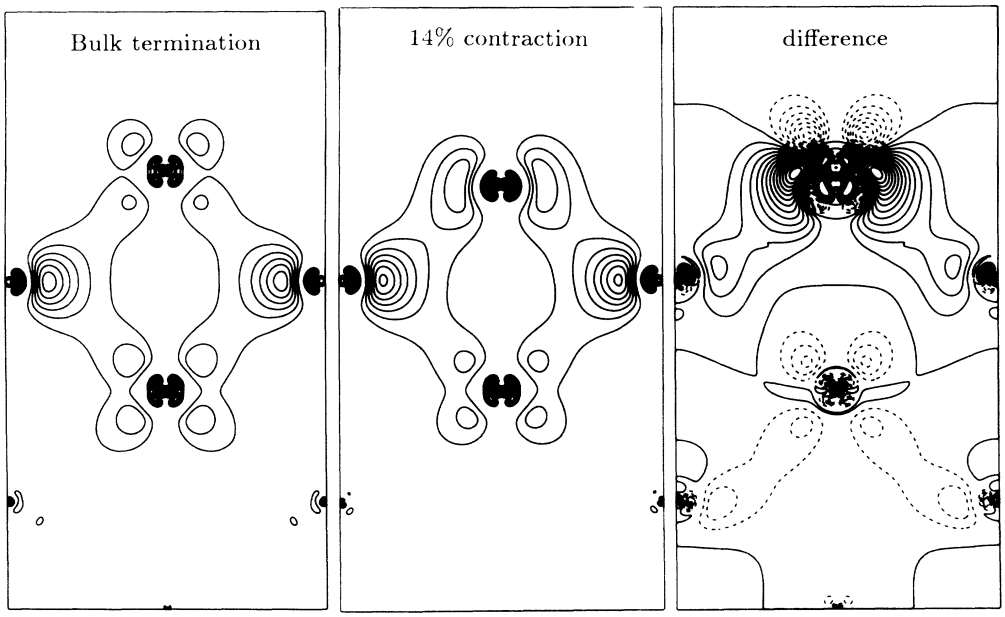

FIG. 12. Single-particle wave functions squared and difference contour plots for the $\bar{\Delta}_2$ surface resonances at the Fermi level in a (110) plane perpendicular to the surface corresponding to bulk-terminated and 14% contracted surfaces. Wave functions are normalized to unity over the nine-layer films; successive contours differ by 10^{-3} electrons/a.u.^{3}. The solid (dotted) difference contours represent increased (decreased) density of the 14% contracted surface relative to the bulk-terminated surface, in units of 2×10^{-4} electrons/a.u.^{3}.

data support a contraction closer to 14% than to 0%.

The $\bar{\Delta}_2$ surface resonances appear to play a role in the large observed relaxation of the surface. The calculated contraction of $\sim 13.2\%$ is large compared to the calculated value[21] of 4% for the unreconstructed W(001) surface. The contraction of the surface has two major effects on the $\bar{\Delta}_2$ resonances: (1) The resonance is pushed to greater binding energy, resulting in increased occupation of the resonance [cf. Figs. 2(a) and 2(b)] and (2) the wave function becomes more bonding between the surface and subsurface layers. In a simple one-particle picture, the first effect suggests increased binding with decreased interlayer separation. For W(001) the corresponding states are completely occupied (as well as not being as localized), thereby contributing a smaller gain in energy with contraction of the surface. From the behavior of the Ta(001) resonances with changes in interlayer separation, these states should be bonding between layers. The calculations show that the states are indeed bonding between the top layers. In Fig. 12, the wave functions squared ($|\psi(\mathbf{r})|^2$) for the $\bar{\Delta}_2$ resonances near E_F are shown in a (110) plane perpendicular to the surface for both the bulk-terminated and 14% contracted surface, as well as the difference between the two. The first point to note is that these states are bonding between the first two layers. (The spectral weight shifts from being mainly on the surface layer near $\bar{\Gamma}$ to being mainly on the subsurface layer at $\bar{X}$.) These states are well localized to the surface region, even though eigenvalues of these states are close to or even overlapping the bulk continuum. While this may at first be surprising, the planar nature of the orbitals allow only weak coupling to the bulk continuum. The difference plot clearly shows a significant buildup of bonding density between the first two layers accompanying the contraction of the surface. This increased density in the surface region comes about by increased localization in the surface region, as seen by the decrease in density in the deeper layers. It is the increased bonding between the uppermost layers for the $\bar{\Delta}_2$ resonances that provides a driving force for the large contraction of the Ta(001) surface.

G. Surface reconstruction

There has been a considerable amount of experimental and theoretical work on the stability of the (001) faces of W and Ta.[1-10,18,19] The LEED experiments show a $c(2\times 2)$ pattern when W(001) is cooled below room temperature or submitted to small amount of hydrogen exposure. It is thought that the reversible temperature-dependent reconstruction results from the formation of zigzag chains of surface atoms, the so-called parallel-shift model, along the $\langle 110 \rangle$ direction. The hydrogen-induced reconstruction is again a parallel shift of surface atoms, but now along the $\langle 100 \rangle$ direction.

Early photoemission studies have shown that W(001) has a number of surface states near the Fermi level.[7,8] Of particular interest is a $\bar{\Sigma}_2$ surface state that crosses the Fermi level approximately halfway to the surface-BZ boundary. This state (and its $\bar{\Sigma}_1$ partner) are generally believed to be responsible for the reconstruction of W(001).

Ta is to the left of W in the Periodic Table with the same bcc lattice structure. The electronic structure of Ta and W is very similar except that the Fermi level for W is about 1.8 eV higher in the d bands than it is in Ta. Previous temperature-dependence experiments do not find a reconstruction of the Ta(001) surface down to a temperature of 15 K. Consistent with this, our hydrogen chemisorption experiments on Ta(001) do not show any LEED patterns other than the (1×1) for H exposures of 0.1 L to saturation coverage. The Ta(001) surface is apparently not unstable with respect to W(001)-type reconstructions.

The $\bar{\Sigma}_2$ surface state that crosses the Fermi level in the case of W(001) is now unoccupied for Ta(001) (Figs. 2 and 3). There are, however, other surface resonances that cut the Fermi level. If simple-minded Fermi-surface nesting were the driving mechanism for the W(001) surface, then reconstruction of the Ta(001) surface should occur: The $\bar{\Sigma}_1$ resonance (Fig. 6) crosses the Fermi level at $\sim\frac{1}{3}$ to $\bar{M}$ and the $\bar{\Delta}_2$ state (Fig. 8) cuts the Fermi level at ~ 0.4 to $\bar{X}$, about as close to halfway as the W(001) $\bar{\Sigma}_2$ state crosses E_F.[8] There are, however, significant differences between Ta(001) and W(001). First of all, for W(001) a surface resonance in an absolute band gap crosses the Fermi level. For the Ta(001) surface, the resonance that crosses the Fermi level is located in a symmetry gap that only exists along $\bar{\Gamma}\rightarrow\bar{X}$.

Since the $\bar{\Sigma}_1$ state is basically a surface-enhanced bulk feature, this state does not provide a driving mechanism for a reconstruction. The $\bar{\Delta}_2$ states, on the other hand, are quite localized, and so a simple Fermi-surface nesting argument would predict a reconstruction in the $\langle 100 \rangle$ direction. The main reason this does not happen is related to the wave-function character (d_{xy} with some d_{yz}) of these resonances. For neither of the Ta(001) resonances does the other symmetry partner exist in the same energy range, nor are the wave-function *shapes* consistent with a reconstruction in the same way as occurs[6] for W(001).

V. SUMMARY AND CONCLUSION

We have performed a systematic study of the electronic structure of Ta(001) using photoemission experiments and local-density calculations. A number of surface resonances on the Ta(001) have been identified throughout the Brillouin zone. The wave-function characters of these surface resonances are determined by utilizing polarization and final-state effects in angle-resolved photoemission. The self-consistent local-density-functional calculations confirm the existence of these surface resonances and their characterization. The agreement for the initial-state properties and dispersion between experiment and theory is best for calculations for a 21-layer Ta(001) slab in which a 14% contraction of the surface is considered.

At the $\bar{\Gamma}$ point, three surface resonances are located at about 0.0, 2.7, and 3.4 eV below the Fermi level. The dispersion of these surface resonances throughout the surface BZ are followed and are identified as derived from the d states of the bulk bands. Both experiment and theory suggest that the resonances at E_F and 2.7 eV are

mainly d_{z^2} in character, while the state at 3.4 eV is composed of both d_{z^2} and $d_{x^2-y^2}$ orbitals.

Total-energy calculations for nine-layer slabs of Ta(001) with various first-layer lattice spacings predict[11] a 13.2% surface-layer contraction. This result is comparable with the recent photoelectron-diffraction determination[12] of the geometry of the Ta(001) surface, which suggest a 10% contraction of the first interlayer spacing. In addition, there is poor agreement between our angle-resolved photoemission data and the calculations assuming bulk-terminated Ta(001). The location and dispersion of all three surface resonances agree well with the calculations for a 21-layer 14% surface-contracted slab, although there remain discrepancies between experiment and theory due to errors in the LDA and to self-energy effects inherent in the excited-state photoemission process.

Perhaps surprisingly, the fully relativistic calculations show that the contribution of spin-orbit coupling for the occupied states of Ta(001) is rather small. Contrary to the case of W(001), the Ta(001) bands which are modified by spin orbit are mostly located above the Fermi level. We are able to interpret all the experimental features in terms of the scalar-relativistic bands for a contracted-surface interlayer separation.

Finally, we note that the surface resonances found on the Ta(001) surface may also have effects on the structural properties of the surface. In contrast to the case of W(001), there are no surface states at the Fermi level that have the correct wave-function shapes or dispersions to induce a surface reconstruction. Instead, the $\bar{\Delta}_2$ surface resonances on Ta(001) provide a driving mechanism for the large surface relaxation.

ACKNOWLEDGMENTS

The authors thank D. Zehner for providing the Ta(001) single crystal for these studies. One of the authors (X.P.) wishes to express his sincere thanks to D. Heskett and G. M. Watson for their assistance. This work was carried out in part at the National Synchrotron Light Source at Brookhaven National Laboratory (Upton, NY). The synchrotron beam line was funded and supported by the National Science Foundation Materials Research Laboratory (NSF/MRL) program under Grant No. DMR-88-19885, and by the Division of Materials Science of the Office of Basic Energy Sciences, U.S. Department of Energy under contract DE-AC05-84OR21400 with Martin Marietta Energy Systems, Inc. One of us (M. W.) was supported by the Division of Materials Sciences of the Office of Basic Energy Sciences, U. S. Department of Energy under Contract No. DE-AC02-76CH00016 and by a grant of computer time at the National Energy Research Supercomputer Center (NERSC).

*Present address: Physical Science Department, IBM Research Division, Almaden Research Center, San Jose, CA 95120-6099.

[1]A. Titov and W. Moritz, Surf. Sci. **123**, L709 (1982).

[2]S. T. Ceyer, A. J. Melmed, J. J. Carroll, and W. R. Graham, Surf. Sci. **144**, L444 (1984).

[3]H. Krakauer, M. Posternak, and A. J. Freeman, Phys. Rev. Lett. **43**, 1885 (1979).

[4]M. Posternak, H. Krakauer, A. J. Freeman, and D. D. Koelling, Phys. Rev. B **21**, 5601 (1980).

[5]X. W. Wang, C. T. Chan, K. M. Ho, and W. Weber, Phys. Rev. Lett. **60**, 2066 (1988).

[6]M. Weinert, A. J. Freeman, and S. Ohnishi, Phys. Rev. Lett. **56**, 2295 (1986).

[7]S.-L. Weng, E. W. Plummer, and T. Gustafsson, Phys. Rev. B **18**, 1718 (1978).

[8]M. I. Holmes and T. Gustafsson, Phys. Rev. Lett. **47**, 443 (1981).

[9]R. A. Bartynski and T. Gustafsson, Phys. Rev. B **35**, 939 (1987).

[10]H. Krakauer, Phys. Rev. B **30**, 6834 (1984).

[11]M. Weinert (unpublished).

[12]R. A. Bartynski, D. Heskett, K. Garrison, G. M. Watson, D. M. Zehner, W. N. Mei, S. Y. Tong, and X. Pan, Phys. Rev. B **40**, 5340 (1989).

[13]D. D. Koelling and B. N Harmon, J. Phys. C **10**, 3107 (1977); T. Takeda, Z. Phys. B **32**, 42 (1978); H. Gollisch and L. Fritsche, Phys. Status Solidi B **86**, 145 (1978).

[14]R. H. Gaylord and S. D. Kevan, Phys. Rev. B **36**, 9337 (1987).

[15]K. Jeong, R. H. Gaylord, and S. D. Kevan, Phys. Rev. B **38**, 10 302 (1988).

[16]J. W. Davenport, M. Weinert, and R. E. Watson, Phys. Rev. B **32**, 4876 (1985).

[17]M. Weinert, E. Wimmer, and A. J. Freeman, Phys. Rev. B **26**, 4571 (1982).

[18]P. Soukiassian, R. Riwan, and J. Lecante, Phys. Rev. B **31**, 4911 (1985).

[19]G. Treglia, M. C. Desjonqueres, and D. Spanjaard, Solid State Commun. **55**, 961 (1985).

[20]L. F. Mattheiss and D. R. Hamann, Phys. Rev. B **29**, 5372 (1984).

[21]C. L. Fu, E. Wimmer, A. J. Freeman, and M. Weinert, Phys. Rev. Lett. **54**, 2261 (1985).